Earth Observation from a High Orbit: Pushing the Limits with Synthetic Aperture Optics

L. M. Mugnier, F. Cassaing, G. Rousset, B. Sorrente

Office National d'Études et de Recherches Aérospatiales
Optics Department / High Resolution Imaging Group
BP 72, 92322 Châtillon cedex, France

Abstract

The resolution of a diffraction limited optical telescope is inversely proportional to its diameter; the latter is limited by the current technology to about 10 meters for ground-based systems, and even more limited by volume and mass constraints for space-based systems. Synthetic Aperture Optics (SAO) is a technique that allows the breaking of this limit; it consists in making an array of telescopes (or of mirrors) interfere, so that the data contains some high resolution information at spatial frequencies given by the separation of the telescopes (or "baseline") rather than by their sizes. In this communication, we first briefly review the two types of SAO instruments (called "Michelson" and "Fizeau") and the possible types of beam combination. We then study the possibility of obtaining wide-field interferometric imaging for a Michelson instrument. Then, we address the problem of optimizing the array configuration, which is an important problem for the design of a SAO instrument. We then give some insight on the image restoration, which is a necessary component of the observation system due to the shape of the PSF of a SAO instrument. We conclude that SAO is a promising technique for high resolution Earth observation, especially from a high orbit such as a geostationary one.

1 Typology of SAO instruments

Two types of optical interferometers (or SAO instruments) exist. A Fizeau interferometer contains a set of mirrors forming a virtually common primary mirror, whose light is combined onto a common secondary mirror (which can itself be segmented). The combination of the light beams coming from each piece of the primary mirror forms an image that is recorded in a common focal plane, in exactly the same way as for a monolithic telescope. The NGST is an example of such an instrument. In contrast, a Michelson interferometer consists of a set of (so-called elementary) telescopes, whose light is brought by a set of periscopes into an additional (so called beam combination) telescope. The interferences are recorded in this beam combination telescope, either in a pupil plane or in a focal plane. The ground-based interferometers built or being built for astronomy are Michelson-type interferometers. Figure 1 shows the two kinds of instruments, for the same input pupil (from [1]).
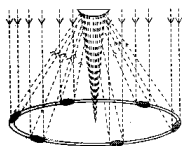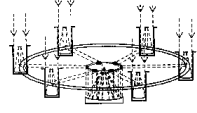

Fizeau	Michelson
Common virtual primary	Elementary telescopes
Focal plane combination: $\Rightarrow$ image formation	Periscopes + interferometer: pupil or focal plane detection

Figure 1: The two types of optical interferometers.

2 Wide-field imaging with SAO instruments

The Fizeau-type instrument is intrinsically an imager and has a wide field of view (FOV), which is limited by the optical design in much the same way as for a monolithic telescope. The Michelson instruments are usually not designed to produce images. In particular, when the data are recorded in a pupil plane, only a discrete set of spatial frequencies of the object (visibilities) is recorded; the field of view is then very limited (risk of field aliasing). In order for a Michelson to produce images, it is necessary to record an image in a focal plane, so that a continuum of spatial frequencies is recorded, and wide field is accessible.

We have studied the conditions under which wide FOV imaging is feasible with a Michelson. It is always possible to cophase at any field position the telescopes of a Michelson by adjusting delay lines and tip/tilt mirrors included for example in the periscopes. For imaging, correct phasing should be simultaneously ensured over a large field. This requires identical aplanetic telescopes, but also new requirements on the optical design.

A famous requirement is homothetic pupil mapping, known as the "golden rule" of SAO [2]: the exit pupil after the telescopes and periscopes should be an exact demagnified replica of the input pupil. For a smaller field, the subpupil demagnification by the telescopes can differ from the baseline demagnification by the periscopes, leading to a "densified pupil" as introduced by Labeyrie [3]. For a larger field, telescope distorsion should also be controlled since the golden rule is only paraxial [4].

The effect of all these aberrations has been evaluated [5]. As expected, it can be shown that the cophasing complexity (i. e. the number and precision of optical parameters to control) increases with the field to resolution ratio, which is the number of resolved elements in the desired field. The results are summarized in Table 1.

This analysis has been applied to the EUCLID RTP 9.2 study on the feasibility of Earth observation with SAO. The simulation of this 3–telescope Michelson instrument with an optical

Table 1: Complexity of an imaging Michelson-type instrument as a function of the field to resolution ratio (FRR).

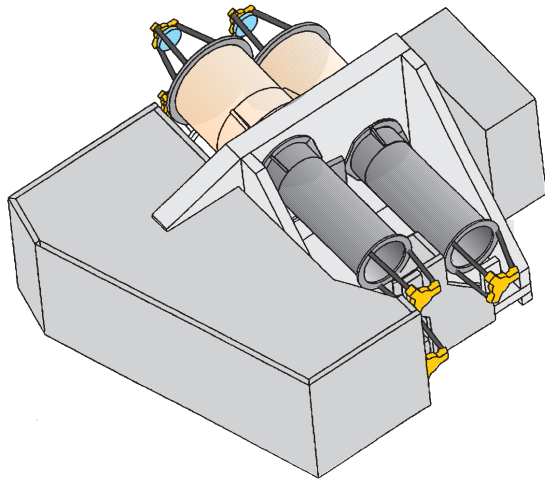| FRR	Optical constraints
≈ 1	relative piston and tilt control
≈ 10	+ lateral base homothecy
≈ 100	+ complete (baseline+diameter) lateral homothecy
≥ 1000	+ longitudinal homothecy, + field curvature and distortion.

Figure 2: Perspective view of a SAO instrument for Earth observation.

design software confirmed that by careful design of the telescopes, a very large field to resolution ratio can be obtained. A perspective view of the instrument is shown in Fig. 2. A thorough simulation of this instrument has been performed, whose results are given in Section 4.

Cophasing such an instrument is a major issue because of the large number of degrees of freedom. The most critical parameters to be controlled are on-axis tip/tilt and piston on each aperture. They are measured by an internal source sensor; this sensor analyzes the diffraction pattern of the 3-beam interferogram given by a point-like source retro-reflected by a common reference plane, which overlaps a small area of each aperture [6]. This setup ensures fast and accurate measurements to correct for instrument vibrations, but can be biased by aperture subsampling or by reference drifts.

The other parameters to be controlled in real-

time are the lateral pupil position and the telescope magnification. Measuring these parameters requires sensors distributed in the whole FOV. Fortunately these parameters are less critical in terms of amplitude and can be measured at a lower frequency, directly on the observed object in order to minimize biases. These so-called external sensors are also used to correct for the slowly evolving bias of the internal sensor.

3 Aperture configuration optimization

The choice of the positioning of the elements of a phased array of optical telescopes is an important point for the preliminary design of a SAO instrument, whether these elements be pieces of a primary mirror (Fizeau) or elementary telescopes (Michelson). A whole body of work exists in the literature on this subject, either based on shaping the PSF of the instrument, or on the idea of uniformity of the frequency coverage.

A more global approach consists in considering together the image acquisition and the restoration, and in optimizing the aperture configuration so that the restored image be as close as possible to the original observed object. This approach is usually referred to a "experiment design" in the signal processing community. Let o be the original object of interest, and $i = h \star o + n$ the recorded image, where h is the PSF of the instrument, $\star$ denotes convolution and n is an additive noise. In order to keep the derivations tractable, the deconvolution is taken as a linear filter g (e.g., an inverse filter truncated to the maximum spatial frequency of interest); the restored image, or estimated object, is then $\hat{o} = g \star i$. If nothing is assumed about the noise statistics, then it can be shown [7] that the aperture configuration that leads to an $\hat{o}$ that is closest to o in the least-squares sense is the one that maximizes the minimum of the transfer function $\bar{h}$ over the frequency domain of interest. One can note that this result gives a frequency-domain optimality condition, but this condition is not imposed *a priori* but, rather, derived from the described global approach, which considers the image restoration as part of the observation
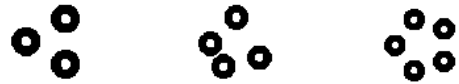

Figure 3: Optimal aperture configurations with 3, 4 and 5 telescopes, for a given collecting surface and resolution.

system.

Figure 3 shows the result of this optimization performed for 3, 4 and 5 elementary telescopes, for a given collecting surface and a given target resolution. The collecting surface is derived from signal-to-noise ratio considerations, and the maximum frequency of interest is derived from mission requirements. One can notice in particular that the four telescopes optimal configuration is not a square, which ensures a better frequency coverage.

4 Image simulation and restoration

Due to the shape of the PSF of a SAO instrument, image restoration is a necessary component of the observation system. The data processing is similar to that of images taken by monolithic telescopes. The transfer function is lower than for a monolithic telescope, but does not go down to zero in the frequency domain of interest when the aperture configuration has been optimized as described in the previous section. The abovementioned Earth observation SAO instrument has been simulated, taking into account the optical and the detector transfer functions as well as photon and detector noises. The optical transfer functions includes design, fabrication and assembly aberrations, as well as cophasing residuals. Figures 4 and 5 show the object used in the simulation and the simulated noisy image respectively.

It is well-known that the restoration of the object using the sole data is an unstable process [8]. It is therefore necessary to add *a priori* information on the solution into the restoration method. This can be done in a Maximum *A Posteriori* (MAP) framework: the object is endowed with an *a priori* distribution $p(o)$, and

Bayes' rule combines the likelihood of the data $p(i|o)$ with this *a priori* distribution into the *a posteriori* probability distribution $p(o|i)$. If the PSF h is perfectly known, then the restored object can be defined as the most probable one given the data: $\hat{o}_{\mathrm{map}} = \arg\max_o p(o|i) = \arg\max_o p(i|o) \times p(o)$. The prior information on the object that is incorporated into $p(o)$ is the available statistical knowledge on its spatial structure, its positivity and possibly its support. With gaussianity and stationarity assumptions both on the object and on the noise, this maximization has an analytical solution, which is the well-known Wiener filter estimate. This estimate is shown in Figure 6; the prior information used consists in a parametric model for the Power Spectral Density (PSD) of the object [9] and the noise variance, which can both be estimated from the image itself by, e.g., the maximum likelihood method. This simulation and restoration have been used to validate the instrument design.

Figure 5: Simulated noisy image.
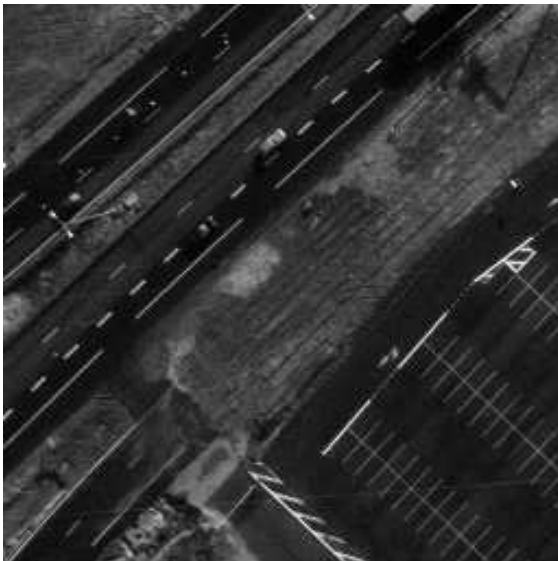

Figure 6: Restored image.

Figure 4: Object used for the simulation.

If one wants to put such a SAO instrument into a high altitude orbit and to keep a high resolution, the size and/or the number of elements of the phased array must be increased. In order to keep these reasonably small, it is worth investigating the possibility to perform some spectral extrapolation from the image, i.e., to restore spatial frequencies that have not been recorded by the instrument.
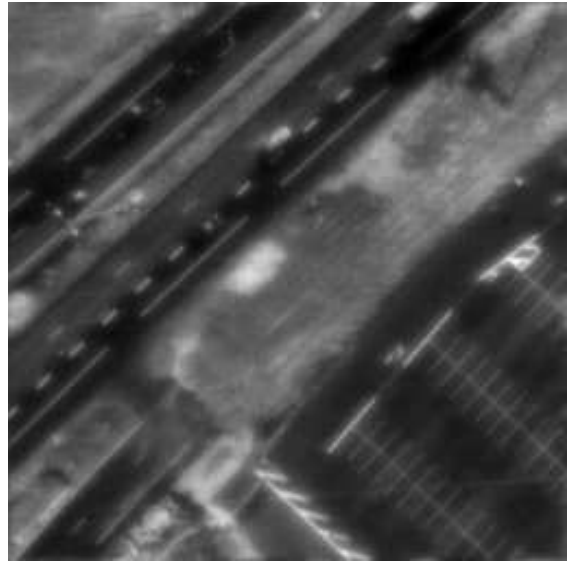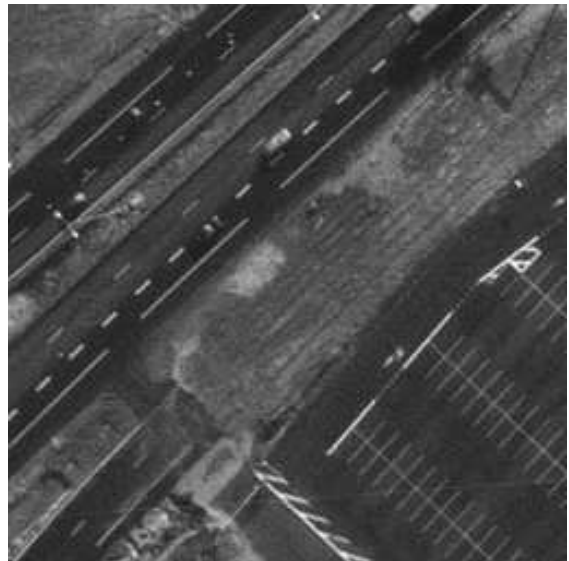
It can be shown that if the models for the object prior probability and for the noise are stationary and Gaussian, such extrapolation is impossible; indeed, the restored image is then a linearly filtered version of the recorded image. One must then resort to more advanced, non-linear restoration methods, which introduce non-gaussianity in the prior (e.g., edge-preserving priors [10–14], entropic priors, etc.) and/or non-stationarity (e.g., object support in-

formation). This has been validated on a one-dimensional simulation of a SAO instrument; figure 7 shows the transfer function corresponding to a two-telescope instrument having zeros before the cutoff frequency (left) and the considered object (right), which has a combination of smooth areas and spikes).
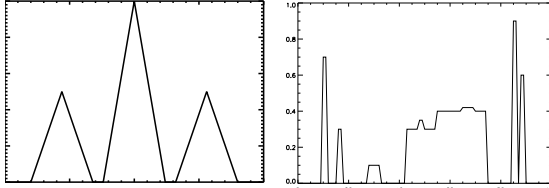

Figure 7: Transfer function of a diluted two-telescope instrument, and object considered for the simulation.

The left part of figure 8 shows the image that would be recorded by such an instrument, with a 1% additive noise. The right part of the same figure shows the restored images obtained with an edge-preserving prior and a prior on the bounds of the object (constrained to be between 0 and 1). The object is quite well restored despite the missing frequencies in the recorded image. The inspection of the Fourier transform of the restored object (see Fig. 9) shows that these missing frequencies have indeed been restored by the use of the edge-preserving prior. One must note that this spectral interpolation (and extrapolation) works well only when the size of the frequency holes to be filled in is relatively small compared to the overall frequency domain of interest [15]. This is illustrated in Figure 10, where the telescope separation has been increased; the object's frequencies lying between the central peak and the interference peak are notably underestimated.

Another advanced image restoration problem of interest for a SAO instrument is the case when the instrument is not perfectly calibrated and the PSF is imperfectly known; this may be due for instance to thermal dilatation or to vibrations. A solution to this problem is known as "myopic deconvolution"; it consists in jointly estimating the object of interest and the PSF; this has already been demonstrated for long exposures in adaptive optics [9, 13] and for short exposures
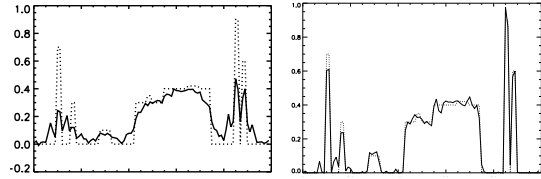

Figure 8: Simulated (left) and restored (right) images. The true object is recalled in dotted line.
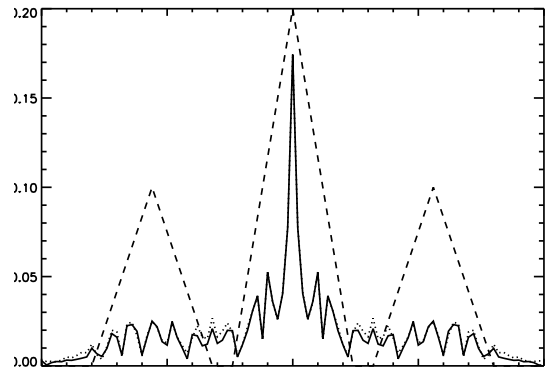

Figure 9: Spectrum of the restored image (continuous line); the spectrum of the true object (dots) and the transfer function (dashed line) are shown for comparison.
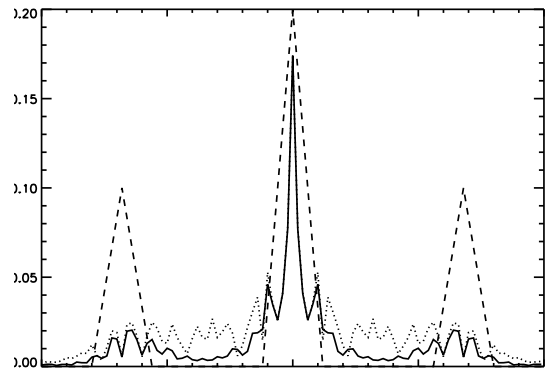

Figure 10: Spectrum of the restored image (continuous line) for an instrument with a very diluted aperture configuration; the spectrum of the true object (dots) and the transfer function (dashed line) are shown for comparison.

in speckle imaging [16, 17] and in deconvolution by wavefront sensing [14]. This myopic deconvolution gives good results provided one has

some information on the PSF and its variability, in order to sufficiently constrain the estimation. For long exposures, this information is for instance the average PSF and the PSD of the PSF (i.e., error bars on the transfer function) [9]. For short exposures, an efficient way to constrain the estimation is to model the PSF though the phase in the pupil [14, 16, 17], which is similar to using phase closure in interferometry with very diluted apertures.

5 Conclusion

In this communication, we have studied the possibility of wide-field imaging with a synthetic aperture optics instrument. We have shown that this possibility exists both for a Fizeau and for a Michelson instrument, a necessary condition being the recording of the data in the focal plane and not in a pupil plane. We have shown some key elements of a study of the design of a Michelson for Earth observation, in particular the possibility and the strategy for wide field cophasing.

We have developed a tool for aperture configuration optimization and we have simulated the whole acquisition and processing chain.

We have also mentioned some possibilities for the processing of images coming from a diluted aperture instrument or from an imperfectly calibrated instrument.

In conclusion, we believe that SAO is a very promising technique for Earth observation from a high-altitude orbit; in particular a SAO instrument on a geostationary orbit would allow the permanent monitoring of a given zone while having a resolution comparable to that of current Low Earth Orbit satellites, as already noted by ONERA in the conclusions of the EUCLID RTP 9.2 project.

As a final note, we would like to point out that in the course of this work, it has become more and more apparent that even the early design of the instrument must incorporate the data processing as a key subsystem of the global observing system, because this processing can have a strong impact on the design.

References

[1] M. Faucherre, F. Merkle, and F. Vakili. Beam combination in aperture synthesis from space: Field of view limitations and (u,v) plane coverage optimization. In Jean-Pierre Swings, editor, *New Technologies for Astronomy*, volume 1130, pages 138–145. Proc. Soc. Photo-Opt. Instrum. Eng., 1989.

[2] W. A. Traub. Combining beams from separated telescopes. *Appl. Opt.*, 25(4):528–532, 1986.

[3] A. Labeyrie. Resolved imaging of extrasolar planets with future 10-100 km optical interferometric arrays. *Astron. Astrophys. Suppl. Ser.*, 118:517–524, September 1996.

[4] T. W. Stuhlinger. All-reflective phased array imaging telescopes. In *International lens design conference*, volume 1354, pages 438–446. Proc. Soc. Photo-Opt. Instrum. Eng., 1990.

[5] F. Cassaing. *Analyse d'un instrument à synthèse d'ouverture optique : méthodes de cophasage et imagerie à haute résolution angulaire*. PhD thesis, Université Paris XI Orsay, December 1997.

[6] F. Cassaing, L. M. Mugnier, G. Rousset, and B. Sorrente. Key aspects in the design of a synthetic aperture optics space telescope for wide field imaging. In N. Duric, editor, *Catching the perfect wave*, number 174 in Pub. Astron. Soc. Pacific, Albuquerque, June 1998.

[7] Laurent Marc Mugnier, Gérard Rousset, and Frédéric Cassaing. Aperture configuration optimality criterion for phased arrays of optical telescopes. *J. Opt. Soc. Am. A*, 13(12):2367–2374, December 1996.

[8] Guy Demoment. Image reconstruction and restoration: Overview of common estimation structures and problems. *IEEE Trans. Acoust. Speech Signal Process.*, 37(12):2024–2036, December 1989.

[9] J.-M. Conan, L. M. Mugnier, T. Fusco, V. Michau, and G. Rousset. Myopic deconvolution of adaptive optics images using object and point spread function power spectra. *Appl. Opt.*, 37(21):4614–4622, July 1998.

[10] P. J. Huber. *Robust statistics*. John Wiley & Sons, 1981.

[11] P. J. Green. Bayesian reconstructions from emission tomography data using a modified EM algorithm. *IEEE Trans. Med. Imag.*, 9:84–93, March 1990.

[12] Charles Bouman and Ken Sauer. A generalized gaussian image model for edge-preserving map estimation. *IEEE Trans. Image Processing*, 2(3):296–310, July 1993.

[13] J.-M. Conan, T. Fusco, L. Mugnier, E. Kersalé, and V. Michau. Deconvolution of adaptive optics images with imprecise knowledge of the point spread fonction: results on astronomical objects. In *Astronomy with adaptive optics: present results and future programs*, Sonthofen, September 1998. ESO/OSA.

[14] L. M. Mugnier, C. Robert, J.-M. Conan, V. Michau, and S. Salem. Regularized multiframe myopic deconvolution from wavefront sensing. In *Propagation through the Atmosphere III*, volume 3763, Denver, CA (USA), July 1999. Proc. Soc. Photo-Opt. Instrum. Eng.

[15] André Lannes, Sylvie Roques, and Marie-José Casanove. Stabilized reconstruction in image and signal processing; part I: Partial deconvolution and spectral extrapolation with limited field. *J. Mod. Opt.*, 34(2):161–226, 1987.

[16] T. J. Schulz. Multiframe blind deconvolution of astronomical images. *J. Opt. Soc. Am. A*, 10(5):1064–1073, 1993.

[17] E. Thiébaut and J.-M. Conan. Strict *a priori* constraints for maximum-likelihood blind deconvolution. *J. Opt. Soc. Am. A*, 12(3):485–492, 1995.